JOURNAL OF SOLID STATE CHEMISTRY 114, 230–235 (1995)

A New Cuprate with Mercury Bilayers: The "2222" Oxide $Hg_{2-x}M_xBa_2Pr_2Cu_2O_{10-\delta}$ (M = Cu, Pr)

M. Huvé, C. Martin, A. Maignan, C. Michel, G. Van Tendeloo,* M. Hervieu, and B. Raveau

*Laboratoire CRISMAT, ISMRA/Université de Caen, Boulevard du Maréchal Juin 14050 Caen Cedex, France; and *University of Antwerp (RUCA) Groenenborgerlaan 171, B-2020 Antwerp, Belgium*

Received January 11, 1994; in revised form April 20, 1994; accepted April 25, 1994

A "2222" cuprate with mercury bilayers $(Hg_{1.5}Cu_{0.2}Pr_{0.3})Ba_2Pr_2Cu_2O_{10-\delta}$, has been synthesized for the first time. It crystallizes in the $P4/nmm$ space group with a = 3.9072(1) Å and c = 17.219(1) Å. The powder XRD and HREM studies of this new cuprate show that its structure consists of an intergrowth of double pyramidal (oxygen-deficient perovskite) copper layers, with double fluorite-type layers and distorted triple rock salt layers (mercury bilayers). The structure of this phase can be deduced from that of the "2212" mercury cuprate $(Hg_{1.5}Cu_{0.2}Pr_{0.3})Ba_2PrCu_2O_{8-\delta}$ by the introduction of one additional $|PrO_2|_\infty$ fluorite layer. The regular stacking of the metallic layer and the uniform cationic distribution in the mercury bilayers are remarkable features of this cuprate. The stabilization of the mercury bilayers by praseodymium and the absence of superconductivity are discussed.

INTRODUCTION

After the discovery of superconductivity at 94 K in the cuprate $HgBa_2CuO_{4+x}$ (1), a large series of mercury-based superconductors were isolated (2–11) with critical temperatures ranging from 30 to 150 K. The structural principle of these phases, like that of other superconducting layered cuprates, consists of an intergrowth of rock-salt-type layers and oxygen-deficient perovskite layers and can be formulated as $(Hg, M)_1A_2Ca_{m-1}Cu_mO_{2m+2+x}$ where M = Pb, Bi, Tl, Pr and A = Ba, Sr. One common feature of the cuprates with pure mercury monolayers (1–4) is that these latter layers are strongly oxygen deficient. The reason for this oxygen deficiency is easily explained by the tendency of mercury to adopt the linear twofold coordination. Consequently, it appears difficult to synthesize similar cuprates involving mercury bilayers. Pure mercury compounds with the general formula $Hg_2A_2Ca_{m-1}Cu_mO_{2m+3+x}$ have indeed never been observed until now. Nevertheless, such mercury-based bilayers were recently evidenced for the first time in the mercury-based cuprate $Hg_{2-x}(Cu, Pr)_xBa_2PrCu_2O_{8-\delta}$ (12). It was shown that the stabilization of such bilayers requires the introduction of a trivalent or tetravalent cation, such as praseodymium, onto calcium sites and partially onto mercury sites in order to reach an oxygen content close to "O_8" in the "2212" structure.

Starting from these observations, the possibility of synthesizing mercury-based cuprates with the "2222" structure should be considered. The latter indeed consists of triple rock salt layers intergrown with oxygen-deficient perovskite layers and double fluorite-type layers. In other words, it is derived from the "1222" structure by replacing double rock-salt-type layers with triple rock-salt-type layers. Only two cuprates, $Bi_2Sr_2(Re_{1-x}Ce_x)Cu_2O_{10}$ (Re = Sm, Eu, or Gd) and $Tl_2Ba_2(Eu_{1.9}Ce_{0.1})Cu_2O_{10}$ (13) have been reported for the "2222" series. In these cuprates as well as in the 1222 structures, the cations located on the cubic sites of the fluorite-type layers are lanthanides.

Thus the present paper deals with the synthesis and characterization of a new mercury-based cuprate with the "2222" structure, $Hg_{2-x}M_xBa_2Pr_2Cu_2O_{10-\delta}$, in which 75% of the mercury sites are occupied by Hg(II) and the remaining 25% are occupied by copper and praseodymium.

CHEMICAL SYNTHESIS AND PHASE IDENTIFICATION

The Hg–Ba–Pr–Cu–O system was investigated on the basis of the nominal composition $Hg_{2-x}M_xBa_2Pr_2Cu_2O_{10}$ corresponding to the existence of mixed mercury bilayers. Taking into account cation size and coordination considerations as well as the results obtained with other mercury compounds (12), we assumed that M should be praseodymium and copper, thus the complex formulation $(Hg_{2-x}Pr_{x-y}Cu_y)Ba_2Pr_2Cu_2O_{10}$ was investigated.

The samples were prepared from mixtures of HgO, BaO_2, Pr_6O_{11}, and CuO ground together in an agate mortar and pressed into bars. They were sealed in silica tubes and heated to 800°C; the temperature was maintained for 8 hr and slowly decreased to room temperature.

The best sample was obtained for x = 0.5 and y = 0.2;

0022-4596/95 $6.00

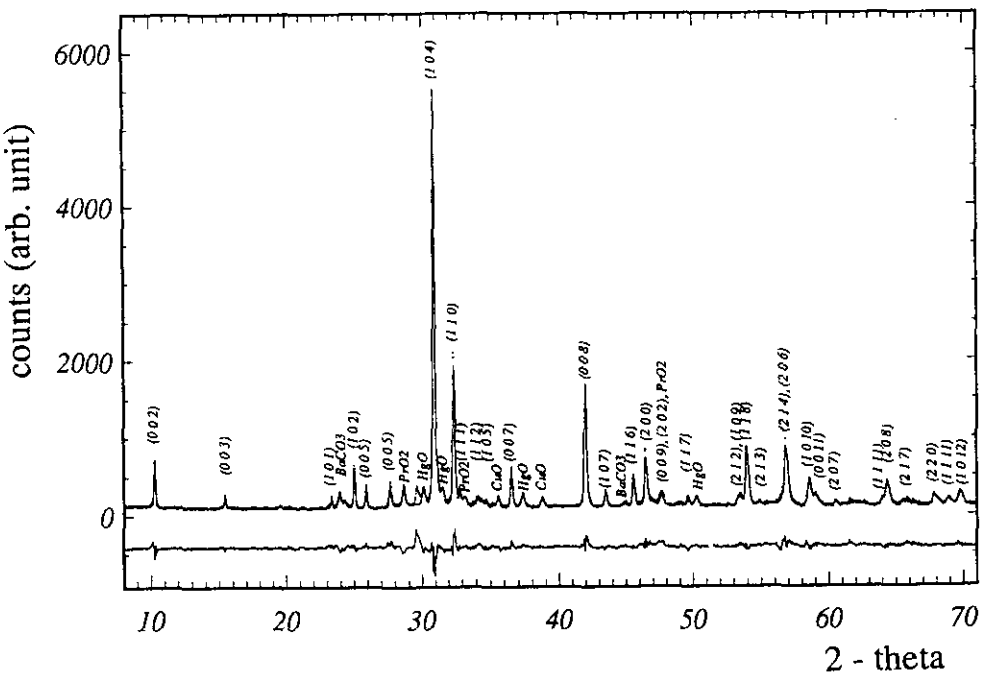

FIG. 1. Observed and calculated X-ray pattern plots in the range $8° \leq 2\theta \leq 71°$ (Cu$K\alpha$ radiation) for $Hg_{1.5}Ba_2Pr_{2.3}Cu_{2.2}O_{10-\delta}$. The difference curve is shown at the bottom of the figure.

the X-ray pattern (Fig. 1), recorded with Cu$K\alpha$ radiation, evidenced an almost pure phase (traces of HgO, PrO_2, CuO, and $BaCO_3$ were found and an unidentifed peak was observed at 30° in 2θ). The reconstruction of the reciprocal space, carried out with a JEOL 200CX electron microscope, showed a tetragonal cell with $a = a_p \approx 3.9$ Å and $c \approx 17.2$ Å. The conditions of reflection are $hk0$: $h + k = 2n$, as shown from [001] and [100] ED patterns in Fig. 2; note that the 010 reflection in Fig. 2b is present, due to double diffraction. The cell parameters were refined from X-ray data to $a = 3.9072(1)$ Å and $c = 17.219(1)$ Å. The EDS analyses performed with a KEVEX analyzer on different crystal fragments show that the cation composition does not vary significantly from one crystal to the other. The new phase can therefore be formulated as $Hg_{1.5}Ba_2Pr_{2.3}Cu_{2.2}O_{10-\delta}$.

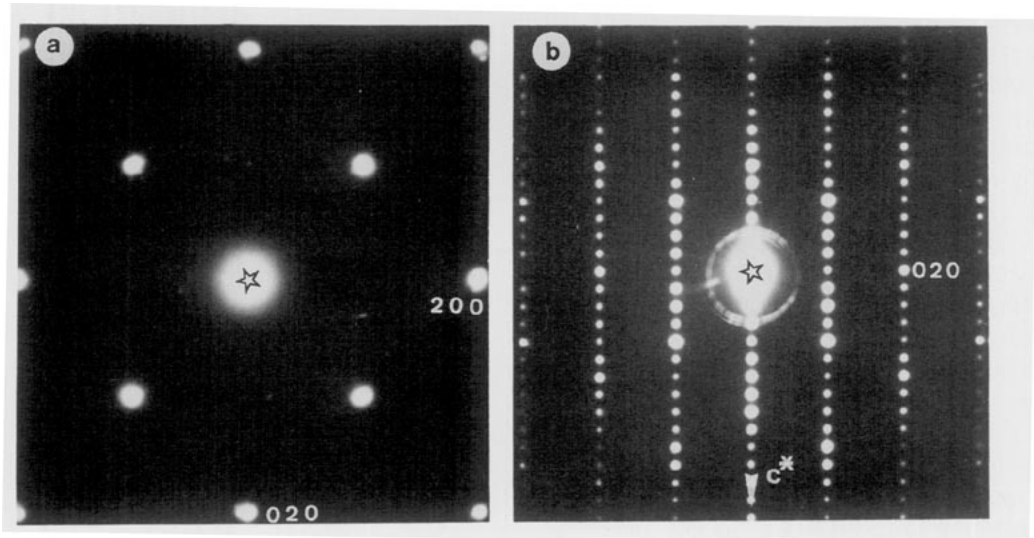

FIG. 2. $Hg_{1.5}Ba_2Pr_{2.3}Cu_{2.2}O_{10-\delta}$ electron diffraction patterns: (a) [001] and (b) [100].

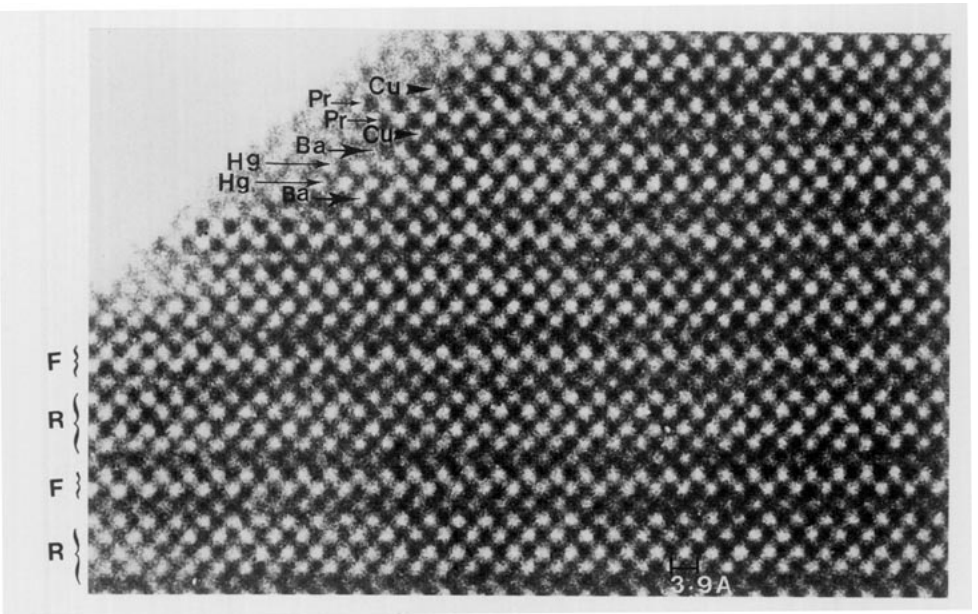

FIG. 3. [100] HREM image allowing deduction of the layer sequence. The columns of heavy atoms are imaged as white dots; the different cations are indicated. F indicates the fluorite-type layers and R the rock-salt-type layers.

HREM CHARACTERIZATION

The layer sequence along the c-axis was studied by high-resolution electron microscopy (HREM) on a TOPCON 002B electron microscope, operating at 200 kV and having a point resolution of 1.8 Å. Figure 3 shows an image along the [100] direction where all cation positions are imaged as bright dots. The 17.2 Å unit cell (outlined in Fig. 3) can clearly be subdivided into two blocks: a block labeled R, consisting of four alternating rows of extra bright dots, and a block, labeled F, consisting of two alternating bright dots. Both blocks are separated by a row of gray dots.

The first block of four layers (R-block) can be associated with the sequence "–BaO–(Hg, M)O_z–(Hg, M)O_z–BaO–." This identification is based on the similarity with images in the related oxides $Tl_2Ba_2Ca_{m-1}Cu_mO_{2m+4}$ (14–15) and on computer simulations based on the structure calculated by X-ray diffraction (see below). On the HREM image at this particular defocus, it is impossible to differentiate between the Ba ions and the Hg ions, but images taken at other defocus values allow one to do so. The $[BaO]_\infty$ layers ensure the junction between the perovskite and the mercury bilayers.

The second block (F-block) is associated with the presence of a $[Pr_2O_2]_\infty$ double layer; this is due to the contrast variations as function of focus and the tendency of the $[Pr_2O_2]_\infty$ layers to adopt a fluorite-type structure. The single rows of less intense white dots between the two blocks are attributed to the $[CuO_2]_\infty$ layers.

We therefore conclude that the sequence of layers along the c-axis should be [BaO–(Hg, M)O_z–(Hg, M)O_z–BaO–CuO_2–Pr–O_2–Pr–CuO_2], which is the "2222" structural type, represented schematically in Fig. 4. Based on this rough model, structural refinements of the positional parameters could for the first time be carried out by X-ray diffraction (see next section). Based on these X-ray-refined atom positions, computer simulations allow one to predict the HREM images for different defocus values; such a set of images for a crystal thickness of 40 Å is reproduced in Fig. 5 for focus values ranging from +200 to −600 Å. They confirm the above interpretation and indicate that the experimental image of

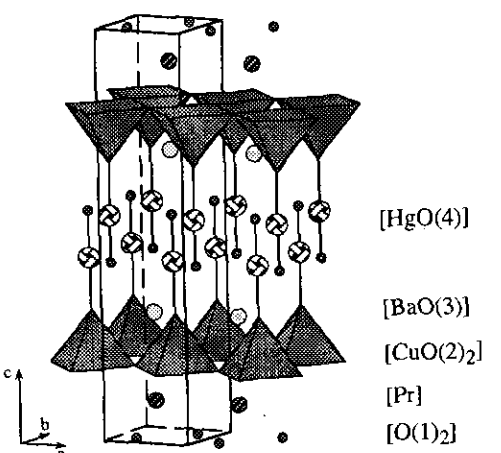

FIG. 4. Schematic representation of the "2222" structure. The HgO_2 sticks are indicated.

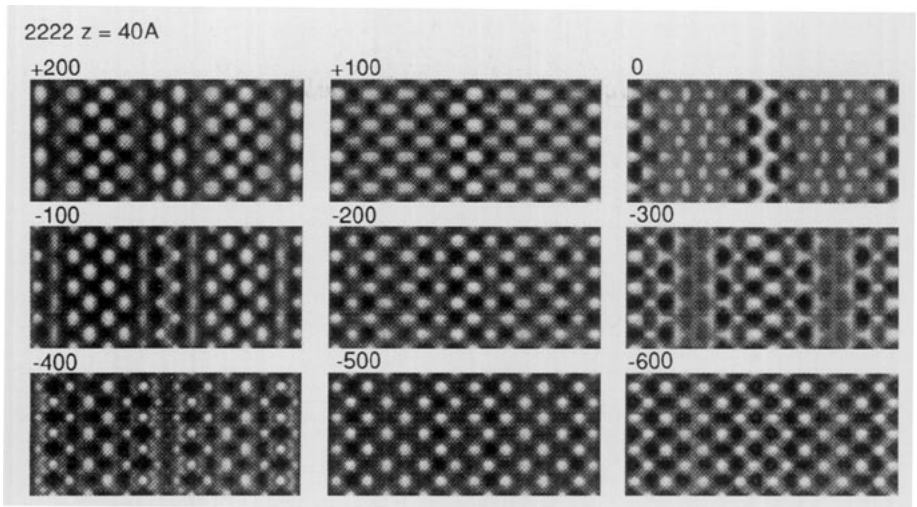

FIG. 5. Computer-simulated [100] images for different focus values (200 Å $\leq \Delta f \leq -600$ Å). The crystal thickness is 40 Å.

Fig. 3 has been recorded for a focus value of +200 Å. Other experimental images are also in agreement with these simulations.

POWDER X-RAY DIFFRACTION STUDY

The X-ray diffraction pattern of this phase was determined with a Philips diffractometer using Cu$K\alpha$ radiation. The structure calculations were carried out using the Rietveld method (program DBW 3.2 (Ref. 16)) in the $P4/nmm$ space group (No. 129) with its origin at the center (115 possible reflections in the range $8 \leq 2\theta \leq 100°$). The starting positional parameters are those of the ideal structure (Fig. 4); they were first refined, and then the thermal factors of the cations (those of oxygens being fixed to 1 Å^2) and their occupancy factors were refined. The R_i factor was lowered to 0.076 for the refined parameters given in Table 1. These results confirm the structural model deduced from the HREM observations. Note that the occupancy factor of the Hg site was refined to 73 ± 3 electrons which is consistent with the EDS analysis (70 electrons). It is also worth pointing out that the cation distribution is similar to that observed for the "2212" oxide (12), with an average composition of $(Hg_{0.75}Pr_{0.15}Cu_{0.10})$ for the mixed mercury layers.

The interatomic distances calculated from the refined positional parameters (Table 2) are close to those usually observed:

—The Hg–O distances are similar to those in the mercury oxide with two short distances along **c** (close to 2 Å) and four long distances in the layer plane (4 × 2.77 Å).

—The barium environment is very regular with none Ba–O distances ranging from 2.7 to 2.8 Å.

—The praseodymium atoms are displaced from the center of the fluorite cage toward the $[CuO_2]_\infty$ layer; such behavior is usually observed in the oxides composed of double fluorite layers (17, 18).

—The CuO_5 pyramids exhibit four short Cu–O distances of 1.95 Å and a long apical distance of 2.38 Å. The copper sites are at the same level as the oxygen of the basal plane.

TABLE 1

Refined Structural Parameters from X-ray Powder Diffraction Data (Space Group, $P4/nmm$; Cell Parameters, a = 3.9072(1) Å and c = 17.2192(6) Å)

	x	y	z	B(Å)^2
Hg[a] (2c)	0.75	0.75	0.4377(3)	1.1(2)
Cu (2c)	0.75	0.75	0.1743(7)	0.1(3)
Ba (2c)	0.25	0.25	0.2916(3)	0.8(2)
Pr (2c)	0.25	0.25	0.0762(3)	0.1(1)
O(1) (2a)	0.25	0.75	0	1
O(2) (4f)	0.75	0.25	0.175(1)	1
O(3) (2c)	0.75	0.75	0.312(2)	1
O(4) (2c)	0.25	0.25	0.448(2)	1

Note. R_p = 9.00%; R_{wp} = 12.45%; R_{exp} = 5.09%; R_i = 7.64%.
[a] τ = 0.94(4).

TABLE 2

Interatomic Distances (in Å)

Hg–O(3)	2.16(4)	×1	Ba–O(2)	2.80(1)	×4
Hg–O(4)	1.97(3)	×1	Ba–O(3)	2.786(5)	×4
Hg–O(4)	2.769(2)	×4	Ba–O(4)	2.69(3)	×1
Cu–O(2)	1.954(0)	×4	Pr–O(1)	2.353(3)	×4
Cu–O(3)	2.38(4)	×1	Pr–O(2)	2.59(1)	×4

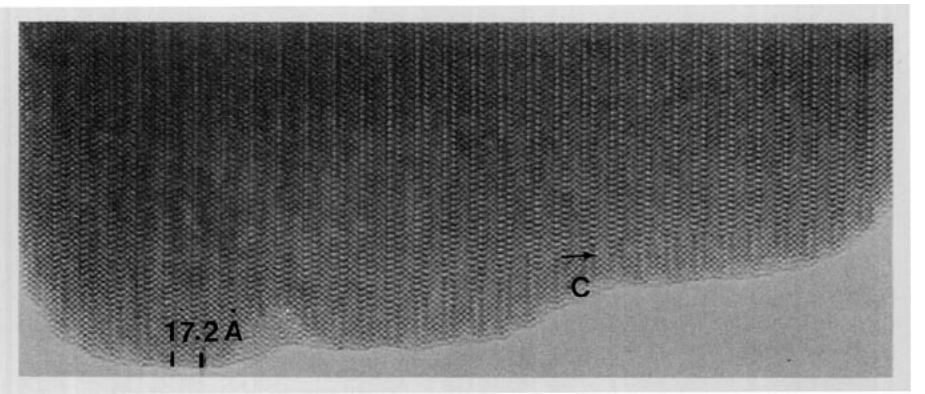

FIG. 6. Lower magnification HREM image showing that the layer stacking along **c** is highly regular.

MICROSTRUCTURE

It is important to note the regularity and perfection of the "2222" stacking over large regions (Fig. 6). Most crystals observed are free of planar defects, which would introduce a sequence different from "2222." Note also the uniformity of the contrast at the level of the $[(Hg, M)O_{1-\delta}]_\infty$ layers, evidencing a statistical distribution of the cations. This can be compared to the regular distribution observed in the "2212" oxide, $Hg_{1.5}Pr_{0.3}Cu_{0.2}Ba_2PrCu_2O_8$ (12), but is opposite to the ordering phenomena observed in the other mixed Hg/Pr strontium cuprates such as "1201," "1212," and "1222" (19). Two factors may explain this different behavior. First, the Hg content is considerably higher in the "2222" and "2212" oxides with Hg/Pr = 5 for the latter instead of 0.67 for the former; second, the size effect of the $[BaO]_\infty$ layers involves a larger perovskite subcell.

In fact, the occasional defects which have been observed are confined to the crystal edges. A typical example is shown in Fig. 7. It shows the presence of a "1222" member in the "2222" matrix, corresponding to the replacement of a mercury bilayer by a mercury monolayer (straight arrow). One also observes the formation of PrO_2 multilayers that are either stacked along **c** on the edge (curved arrow) or connected to $[CuO_2]_\infty$ layers along **b** (upper arrow indicating the fluorite-type layers "F"). Such defects were previously observed in "1222" cuprates involving double fluorite-type layers.

TRANSPORT PROPERTIES

No superconducting properties were observed at temperatures down to 4.2 K, neither by magnetic susceptibility measurements nor by resistivity measurements. At room temperature, the resistivity is close to 5.10^3 Ω cm and is increased by one order of magnitude at 240 K, showing a semiconducting behavior. Below 240 K, the resistivity becomes too high to be measured in our experimental conditions.

The absence of superconductivity in this compound is not unexpected if we consider the valence states of the elements. Praseodymium takes easily the mixed valence Pr(III)/Pr(IV) which can be favored by the synthesis con-

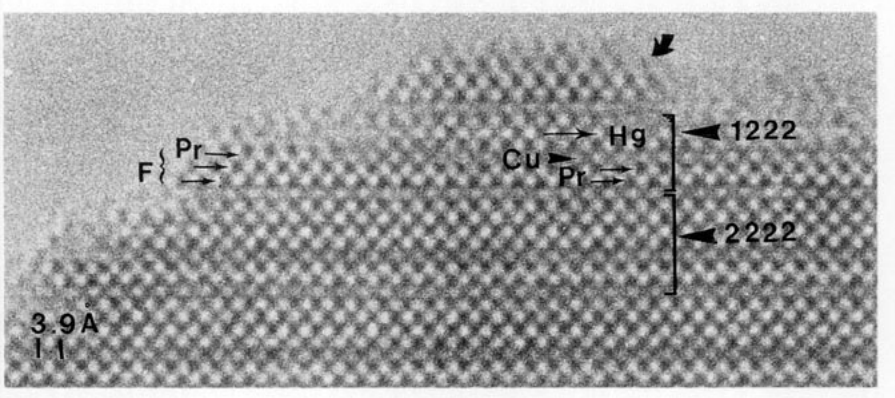

FIG. 7. [100] image showing the existence of different types of defects: a 1222 defective member is observed; at the crystal edge, $[PrO_2]_\infty$ multilayers are stacked (curved arrows); to the left of the image, three praseodymium layers are stacked (instead of two in the normal structure) but the upper layer is connected to a copper layer.

ditions under oxygen pressure and would involve copper mainly in the divalent state according to the oxygen stoichiometry. This is in agreement with the high resistivity of the sample. Moreover, most of the cuprates that exhibit double fluorite-type layers were found to be nonsuperconducting or superconducting with low superconducting volume fractions. The difficulty in inducing superconductivity in such structures is probably associated with the large distance between two successive $[CuO_2]_\infty$ layers due to the introduction of insulating double fluorite layers $[Ln_2O_2]_\infty$.

CONCLUSION

A "2222" cuprate with mercury bilayers, $(Hg_{1.5}Cu_{0.2}Pr_{0.3})Ba_2Pr_2Cu_2O_{10-\delta}$, has been synthesized for the first time. The chemical composition of this phase, whose structure is derived from that of the "2212" mercury cuprate (12) by introducing one additional $[PrO_2]_\infty$ fluorite layer, indicates that praseodymium seems to play a prominent role in the stabilization of mercury bilayers. This can be explained by its high oxidation states Pr(III)/Pr(IV) that allow a sufficient oxygen content to be introduced into the mercury bilayers, so that they are stabilized. Such a situation can be reached due to the ability of praseodymium and copper to partially replace mercury; praseodymium also ensures the formation of double fluorite-type layers. A filling of the mercury layers by oxygen leads mercury to a "2 + 4" coordination, with two apical short bonds (1.97–2.10 Å) forming $Hg^{II}O_2$ sticks and four equatorial long Hg–O bonds (2.76 Å), characteristic of the environment of Hg(II) in HgO (20). The regular stacking of the different layers and the high degree of perfection of the structure are remarkable features. Note also the statistically uniform distribution of Hg, Pr, and Cu at the level of the mercury bilayers, similar to the situation in the "2212" cuprate $(Hg_{1.5}Pr_{0.3}Cu_{0.2})Ba_2PrCu_2O_{8-\delta}$ (12). This is different from the ordering phenomena between Pr and Hg observed in other "Hg–Pr" cuprates (19) that contain, however, significantly more praseodymium in the mixed layers.

REFERENCES

1. S. N. Putilin, E. V. Antipov, O. Chmaissem, and M. Marezio, *Nature* **362,** 226 (1993).
2. A. Schilling, M. Cantoni, J. D. Guo, and H. R. Ott, *Nature* **363,** 56 (1993).
3. S. N. Putilin, E. V. Antipov, and M. Marezio, *Physica C* **212,** 266 (1993).
4. M. Nuñez-Regueiro, J. L. Tholence, E. V. Antipov, J. J. Caponi, and M. Marezio, *Science* **262,** 97 (1993).
5. M. Huvé, C. Martin, G. Van Tendeloo, A. Maignan, C. Michel, M. Hervieu, and B. Raveau, *Solid State Commun.* **90,** 37 (1994).
6. S. F. Hu, D. A. Jefferson, R. S. Liu, and P. P. Edwards, *J. Solid State Chem.* **103,** 280 (1993).
7. R. S. Liu, D. S. Shy, S. F. Hu, and D. A. Jefferson, *Physica C* **216,** 237 (1993).
8. F. Goutenoire, P. Daniel, M. Hervieu, G. Van Tendeloo, C. Michel, A. Maignan, and B. Raveau, *Physica C* **216,** 243 (1993).
9. D. Pelloquin, C. Michel, G. Van Tendeloo, A. Maignan, M. Hervieu, and B. Raveau, *Physica C* **214,** 87 (1993); D. Pelloquin, M. Hervieu, C. Michel, G. Van Tendeloo, A. Maignan, and B. Raveau, *Physica C* **216,** 257 (1993).
10. R. S. Liu, S. F. Hu, D. A. Jefferson, P. P. Edwards, and P. D. Huneyball, *Physica C* **205,** 206 (1993).
11. M. Hervieu, G. Van Tendeloo, A. Maignan, C. Michel, F. Goutenoire, and B. Raveau, *Physica C* **216,** 264 (1993).
12. C. Martin, M. Hervieu, G. Van Tendeloo, F. Goutenoire, C. Michel, A. Maignan, and B. Raveau, *Solid State Commun.*, in press.
13. Y. Tokura, T. Arima, H. Takagi, S. Uchida, T. Ishigaki, K. Asano, R. Beyers, A. I. Nazzal, P. Lacorre, and J. B. Torrance, *Nature* **342,** 890 (1989).
14. M. Hervieu, C. Martin, J. Provost, and B. Raveau, *J. Solid State Chem.* **76,** 419 (1988).
15. M. Verwerft, G. Van Tendeloo, and S. Amelinckx, *Physica C* **156,** 607 (1988).
16. D. B. Wiles and R. A. Young, *J. Appl. Crystallog.* **14,** 149 (1981).
17. R. S. Liu, M. Hervieu, C. Michel, A. Maignan, C. Martin, B. Raveau, and P. P. Edwards, *Physica C* **197,** 131 (1992).
18. R. Vijayaraghavan, C. Michel, A. Maignan, M. Hervieu, C. Martin, B. Raveau, and C. N. R. Rao, *Physica C* **206,** 81 (1993).
19. G. Van Tendeloo, M. Hervieu, X. F. Zhang, and B. Raveau, submitted for publication.
20. K. Aurivillius, *Acta Crystallogr.* **9,** 685 (1956).